JH ~1
13486

P 25

NASA
Technical
Memorandum

NASA TM-103534

/

PARAMETRIC STUDY IN WELD MISMATCH OF
LONGITUDINALLY WELDED SSME HPFTP INLET

By J.B. Min, K.L. Spanyer, and R.M. Brunair

Structures and Dynamics Laboratory
Science and Engineering Directorate

April 1991

NASA
National Aeronautics and
Space Administration

George C. Marshall Space Flight Center

MSFC - Form 3190 (Rev. May 1983)

NASA National Aeronautics and Space Administration	Report Documentation Page		
1. Report No. NASA TM-103534	2. Government Accession No.	3. Recipient's Catalog No.	
4. Title and Subtitle Parametric Study in Weld Mismatch of Longitudinally Welded SSME HPFTP Inlet		5. Report Date April 1991	
		6. Performing Organization Code	
7. Author(s) J.B. Min, K.L. Spanyer, and R.M. Brunair*		8. Performing Organization Report No.	
		10. Work Unit No.	
9. Performing Organization Name and Address George C. Marshall Space Flight Center Marshall Space Flight Center, Alabama 35812		11. Contract or Grant No.	
		13. Type of Report and Period Covered Technical Memorandum	
12. Sponsoring Agency Name and Address National Aeronautics and Space Administration Washington, DC 20546			
		14. Sponsoring Agency Code	

15. Supplementary Notes

Prepared by Structures and Dynamics Laboratory, Science and Engineering Directorate.

*Sverdrup Technology, Inc.

16. Abstract

Welded joints are an essential part of pressure vessels such as the space shuttle main engine (SSME) turbopumps. Defects produced in the welding process can be detrimental to weld performance. Recently, review of the SSME high pressure fuel turbopump (HPFTP) titanium inlet x rays revealed several weld discrepancies such as penetrameter density issues, film processing discrepancies, weld width discrepancies, porosity, lack of fusion, and weld offsets. Currently, the sensitivity of welded structures to defects is of concern. From a fatigue standpoint, weld offset may have a serious effect since local yielding, in general, aggravates cyclic stress effects. Therefore, the weld offset issue is considered in this report. Using the finite element method and mathematical formulations, parametric studies were conducted to determine the influence of weld offsets and a variation of weld widths in longitudinally welded cylindrical structures with equal wall thicknesses on both sides of the joint. From the study, the finite element results and theoretical solutions are presented.

17. Key Words (Suggested by Author(s)) welded joints, SSME turbopumps, weld offsets, parametric study, finite element analysis		18. Distribution Statement Unclassified – Unlimited	
19. Security Classif. (of this report) Unclassified	20. Security Classif. (of this page) Unclassified	21. No. of pages 25	22. Price NTIS

TABLE OF CONTENTS

LIST OF ILLUSTRATIONS

LIST OF TABLES

v

TECHNICAL MEMORANDUM

PARAMETRIC STUDY IN WELD MISMATCH OF LONGITUDINALLY WELDED SSME HPFTP INLET

SUMMARY

Welded joints are an essential part of pressure vessels such as the space shuttle main engine (SSME) turbopumps. Defects produced in the welding process can be detrimental to weld performance. Recently, review of the SSME high pressure fuel turbopump (HPFTP) titanium inlet x rays revealed several weld discrepancies such as penetrameter density issues, film processing discrepancies, weld width discrepancies, porosity, lack of fusion, and weld offsets. Currently, the sensitivity of welded structures to defects is of concern. From a fatigue standpoint, weld offset may have a serious effect since local yielding, in general, aggravates cyclic stress effects. Therefore, the weld offset issue is considered in this report. Using the finite element method and mathematical formulations, parametric studies were conducted to determine the influence of weld offsets and a variation of weld widths in longitudinally welded cylindrical structures with equal wall thicknesses on both sides of the joint. From the study, the finite element results and theoretical solutions are presented.

INTRODUCTION

As the application of welded titanium structures in the aerospace industry is increasing, extensive experimental data are required to characterize typical weld defects encountered in production and to determine their effects on weldments. Recently, review of SSME HPFTP titanium inlet x rays revealed several discrepancies such as penetrameter density issues, film processing discrepancies, weld width discrepancies, porosity, lack of fusion, and weld offsets. The fabrication problems have been associated with the local stress levels due to these defects between the components from which the SSME HPFTP is manufactured. As a result of issues which have arisen concerning the structural analysis applied to evaluate the SSME HFPTP titanium inlet welds, an in-house task has been initiated at NASA/Marshall Space Flight Center. The purpose of the task is to (1) verify the adequacy of the Rocketdyne porosity specification as applicable to the HPFTP titanium inlet, (2) validate the Rocketdyne rationale and fatigue analysis for porosity utilized for material reviews (MR's), and (3) perform a porosity sensitivity study at the most critical weld locations to understand the effect of pore sizes, clusters, location of pores in welds, wall thickness, and weld offset on the structural adequacy of the inlet. The structural integrity evaluation of a welded joint is not a simple process because of complications due to component geometry, defects, and the gradient of material properties across the weld metal, heat-affected zone, and parent metal which result in nonuniform deformations. Although the structural integrity evaluation must include all these factors, only the weld offset issue is considered in this report. If pressure vessels are made of welded elements, there arises the possibility of local stress concentrations due to offsets caused by weld mismatch. These may give rise to relatively high local stresses which may lead to early

failure of the pressurized structures. In this study, a case has been considered under the assumptions that the cylinder has a very large radius, and weld mismatch is localized and only extends for a short distance along the circumferential direction of the cylinder. With these assumptions, the flat plate specimens containing an offset and being loaded in tension are considered. The finite element analysis and theoretical analysis were conducted to determine the influence of weld offset and a variation of weld width in a longitudinally welded cylindrical structure with equal wall thicknesses on both sides of the joint. As a result, the stress concentration factors due to weld offset in a flat plate loaded in tension with various mismatches are presented in this report.

FINITE ELEMENT ANALYSIS

In the current analysis, plate idealization of the longitudinal weld in the straight cylinder, assuming that the applied load is resisted predominantly by the inplane stressing of the shell, is used for analyzing weld offsets subjected to axial loading in tension with a force P as shown in figure 1. Since the membrane stress is very much larger than the bending stress as $t/2r << 1$ (r represents the radius of cylinder), the flat plate model could be considered [1]. Mismatch between components of flat plates can result in substantial local increases in stress. That is, if a butt weld in a flat plate structure under tension is mismatched, an offset is produced which causes bending stresses at the weld in addition to the tensile stresses. Thus, to estimate the effects of parameters considered in weld offsets, an analysis was conducted using a flat plate idealization of the joint geometry at the section of weld offset. ANSYS plane strain finite element models [2] were constructed to perform a parametric study to determine the effect of weld offsets. The finite element model includes weld metal and parent metal regions. The representative finite element model is shown in figure 2. The mesh is more refined in the vicinity of a junction between weld metal and parent metal because of the local variation in stress expected in this region. Dimensions of the analysis models to obtain an offset stress concentration factor (K_{off}) are shown in table 1. In this table L, e, t, and υ represent weld width, weld offset, wall thickness, and Poisson's ratio, respectively. Practically, it is recognized that the case of more than 100-percent mismatch appears. However, in this study mismatches up to 60 percent have been tested. It is only considered that a flush weld bead would be at such a seam to act as a transition section, and that there is no discontinuity of meridian slope, but an eccentricity between the middle surfaces on the two sides of the discontinuity is included. Stress concentrations resulting from reduced thickness or reentrant corners are not considered in determining the stress concentration factors.

THEORETICAL ANALYSIS

If a long cylinder with very large radius-to-thickness ratios and mismatch between shell elements of the same thickness and slope is considered, the plane strain assumption could be made using a flat plate with a mismatched welded joint loaded in tension. Sechler [3] used the same assumption and showed that if the small element $ABCD$ in figure 3 is assumed to be rigid and to rotate as a solid body under the action of the two plate elements attached to it, the problem resolves itself into two parts as follows.

(1) Moment and force equilibrium of the offset element *ABCD*

If the offset is e and the length of the weld width is L, then the equilibrium of the element is given by

$$2PR \cos (\alpha + \beta) - 2SR \sin (\alpha + \beta) - 2M = 0 \quad , \tag{1}$$

or

$$PR \ (\cos \beta \cos \alpha - \sin \beta \sin \alpha) - SR \ (\sin \alpha \cos \beta + \cos \alpha \sin \beta) - M = 0 \quad , \tag{2}$$

where P, S, and M stand for axial tensile load, end shear, and end moment, respectively.

Here

$$\sin \beta = \frac{L}{2R} \quad \text{and} \quad \cos \beta = \frac{e}{2R} \quad ,$$

where R is the diagonal of the small element *ABCD*.

Assuming α is small,

$$\sin \alpha \cong \alpha \quad \text{and} \quad \cos \alpha \cong 1 \quad .$$

Then equation (1) becomes

$$P(e - L\alpha) - S(L + e\alpha) - 2M = 0 \quad , \tag{3}$$

(2) A beam column problem for the two sheet elements *AG* and *CE*, consisting of a cantilever beam with an end shear S, an axial tensile load P, and an end moment M

The cantilever beam is considered as shown in figure 4. The basic equation is

$$EI \ \frac{d^2y}{dx^2} = Sx - P(y_0 - y) - M \quad , \tag{4}$$

where the direction of positive moment is clockwise.

This has a solution

$$y = c_1 \sinh kx + c_2 \cosh kx - \frac{Sx}{P} + y_0 + \frac{M}{P} \quad , \tag{5}$$

where

$$k = \sqrt{\frac{P}{EI}} \quad . \tag{6}$$

Using the boundary condition that $y = (dy/dx) = 0$ at $x = l$ and that $EI(d^2y/dx^2) = -M$ and $y = y_0$ at $x = 0$.

$$y(x) = \left(\frac{S}{Pk \cosh \lambda} + \frac{M}{P} \tanh \lambda \right) \sinh kx - \frac{M}{P}(\cosh kx - 1) - \frac{Sx}{P}$$

$$+ \frac{S}{Pk}(\lambda - \tanh \lambda) - \frac{M}{P}(1 + \sinh \lambda \tanh \lambda - \cosh \lambda) \quad , \tag{7}$$

$$y(0) = \frac{S}{Pk}(\lambda - \tanh \lambda) - \frac{M}{P}(1 + \sinh \lambda \tanh \lambda - \cosh \lambda) \quad , \tag{8}$$

$$\frac{dy}{dx}(x) = \left(\frac{S}{P \cosh \lambda} + \frac{Mk}{P} \tanh \lambda \right) \cosh kx - \frac{Mk}{P} \sinh kx - \frac{S}{P} \quad , \tag{9}$$

$$\frac{dy}{dx}(0) = \frac{S}{P}\left(\frac{1}{\cosh \lambda} - 1 \right) + \frac{Mk}{P} \tanh \lambda \quad ,$$

where

$$\lambda = kl = l\sqrt{\frac{P}{EI}} \quad . \tag{11}$$

From figure 3 it is observed that

$$y(0) \cong R\alpha \sin \beta = R\alpha \frac{L}{2R} = \frac{\alpha L}{2} \quad , \tag{12}$$

and

$$\alpha = \frac{dy}{dx}(x=0) \quad .$$

4

(3) Equation for stress concentration factor due to weld offset

The following equations are derived from equations (3), (8), and (10),

$$P(e - L\alpha) - S(L + e\alpha) - 2M = 0 \quad , \tag{13}$$

$$\frac{\alpha L}{2} = \frac{S}{Pk} (\lambda - \tanh \lambda) - \frac{M}{P} (1 + \sinh \lambda \tanh \lambda - \cosh \lambda) \quad , \tag{14}$$

$$\alpha = \frac{S}{P} \left(\frac{1 - \cosh \lambda}{\cosh \lambda} \right) + \frac{Mk}{P} \tanh \lambda \quad , \tag{15}$$

which are to be solved for α, S, and M in terms of P. Since the most serious problems arise from high stresses (P large) and, in most practical cases, l is relatively large, then $\lambda = l (P/EI)^{1/2}$ will be sufficiently large (>4) so that the following approximations are justified:

$$\sinh \lambda \cong \cosh \lambda >> 1 \quad , \tag{16}$$

$$\tanh \lambda \cong 1 \quad . \tag{17}$$

Equations (13), (14), and (15) then reduce to

$$P(e - L\alpha) - S(L + e\alpha) - 2M = 0 \quad , \tag{18}$$

$$\frac{\alpha L}{2} = \frac{S}{Pk} (\lambda - 1) - \frac{M}{P} \quad , \tag{19}$$

$$\alpha = -\frac{S}{P} + \frac{Mk}{P} \quad . \tag{20}$$

Solving simultaneously,

$$S = Mk \frac{\lambda + 2}{\lambda + 2\lambda - 2} \quad , \tag{21}$$

$$\alpha = \frac{2Mk}{P} \frac{\lambda - 2}{\lambda + 2\lambda - 2} \quad , \tag{22}$$

5

$$Pe = M(\Lambda+2) \left[1 + \frac{2Me}{EI} \frac{\lambda-2}{(\Lambda+2\lambda-2)^2} \right], \tag{23}$$

where

$$\Lambda = Lk = L \sqrt{P/EI} . \tag{24}$$

Detailed study indicates that the last term in equation (23) is negligible, therefore

$$M = \frac{Pe}{\Lambda+2} , \tag{25}$$

$$S = \frac{Pek}{\Lambda+2\lambda-2} , \tag{26}$$

$$\alpha = \frac{2 \ ke(\lambda-2)}{(\Lambda+2)(\Lambda+2\Lambda-2)} . \tag{27}$$

The maximum bending stress due to M is

$$\sigma_b = (+/-) \frac{M \ (t/2)}{t^3/12} = (+/-)\frac{6M}{t^2} . \tag{28}$$

The direct stress is

$$\sigma_0 = \frac{P}{A} = \frac{P}{t} , \tag{29}$$

where A is the area.

Thus, the maximum total stress is

$$\sigma_T = \sigma_0 + \sigma_b = \frac{P}{t} + \frac{6M}{t^2} . \tag{30}$$

The stress concentration factor due to weld offset is therefore given by

$$K_{off} = \frac{\sigma_T}{\sigma_0} = 1 + \frac{6M}{Pt} = 1 + \frac{3(e/t)}{(L/t) \ \rho + 1} , \tag{31}$$

6

where

$$\rho \;=\; k(t/2)$$

$$=\; \frac{t}{2}\;\sqrt{P/EI}$$

$$=\; \frac{t}{2}\;\sqrt{\frac{\sigma_0\, t}{(Et^3)/(12(1-\nu^2))}}$$

$$=\; \sqrt{(3(1-\nu^2)\sigma_0)/E} \quad . \tag{32}$$

Sechler's expression (equation (31)) accounts for the reduction of transverse deformation due to in-plane tensile loading, often called the stress stiffening or geometric stiffening effect. This is more apparent if equation (31) is rearranged as

$$K_{off} \;=\; 1 + 3(e/t)(1/(L\rho/t + 1)) \quad , \tag{33}$$

where the $L\rho/t$ quantity, when factored on the e/t term, accounts for the stress stiffening. Note that Sechler uses the plate flexural rigidity $(Et^3/12(1-\nu^2))$ in the expression for ρ (equation (32)), making K_{off} a function of Poisson's ratio, and that by including the stress stiffening effect, his expression is nonlinear. In this study, a strain (σ_0/E) of 0.25 percent was used as a minimal strain for the HPFTP inlet longitudinal welds. A higher strain would make the Sechler curves in the results section of this paper conservative.

If the stress stiffening effects are ignored or assumed negligible, equation (33) reduces to

$$K_{off} \;=\; 1 + 3(e/t) \quad , \tag{34}$$

which is the standard, small defection, linear formulation commonly used for K_{off} estimation of longitudinal weld mismatch.

RESULTS AND CONCLUSIONS

Analyses were performed for various ratios of weld width (L/t) with 20-, 40-, and 60-percent weld offsets. Initially, the analysis was performed varying offset for a constant weld width $(L/t = 2.86)$. As can be seen in figure 5, the increase in stress is almost proportional to the amount of mismatch. That is, if the weld offset is increased, then the stress concentration factor

(K_{off}) is also increased as expected. The results were compared to the conservatively used results [4]. Generally, if K_{off} is calculated using axial stresses, the values are much higher than those calculated using effective stresses. Also, a comparison shows that the currently used values are the highest and that the values from a finite element model with 60-percent offset has a good correlation with the theoretical value.

In figures 6, 7, and 8, it can be observed that if the weld width is increased then K_{off} is decreased. For $L/t = 1.0$, K_{off} calculated by an axial stress component from the finite element analysis is higher than currently used K_{off}. Consequently, it is believed that an excessive weld width does not adversely affect the structural capability of the joint. A wide weld bead would have a lower K_{off} than a narrow bead of the same amount of offset. The wide welds are therefore structurally acceptable.

The variation of Poisson's ratio was also tested as shown in figures 5 and 9 with the same conditions since a formulation, $K_{off} = 1 + 3\,(e/t)$, for the longitudinal weld cases is currently used [4]. This implies that the weld stiffness effects could be negligible. However, as can be seen in table 2 and figures 5 and 9, if the effective stresses are considered, the values of cases with $\upsilon = 0.3$ are very different from the models with $\upsilon = 0.0$. On the other hand, if axial stresses are compared, the differences are minor. In theoretical analysis, since the values are calculated based on the axial stresses, the theoretical values show the same characteristics as the cases of the finite element axial stresses. However, it is noted that the values from the effective stresses with $\upsilon = 0.3$ are lower than those with $\upsilon = 0.0$. But, the values from axial stresses and theoretical stresses with $\upsilon = 0.3$ are higher than those with $\upsilon = 0.0$. The comparison was also made for the different offset ratio (e/t) with a various ratio of weld width-to-wall thickness (L/t) for $\upsilon = 0.0$ and $\upsilon = 0.3$ in figures 6 to 8 and 10 to 12. As can be observed in these figures, regardless of a change of Poisson's ratio and an amount of offset, the results show that as the bead width is increased the stress concentration factor is decreased. It should be noted that if the weld width is increased, accuracy of the currently used results is decreased. Consequently, since the maximum distortion energy theory (Von Mises yield criterion) to predict onset of plastic flow is the most accepted yield criterion for a material with a reasonable amount of ductility, the effect of Poisson's ratio has to be taken into account in calculating the stress concentration factors in terms of effective stresses for a longitudinal weld case.

The results of the material discontinuity study between the weld metal (E_1) and the parent metal (E_2) are presented in figures 13 through 16 with a ratio of E_1/E_2 equal to 1.0, 1.1, 1.2, and 1.3. For this study, the models were constructed with variations of L/t equal to 1, 2, 3, and 4 for a constant weld offset (40 percent). As can be seen in these figures, the effect of a material difference between the weld area (E_2) and the parent metal area (E_1) could be considered negligible. It is once again observed in these figures that for small L/t ratios the stress factors obtained by finite element analysis are more conservative than currently used values.

DISCUSSION

In order to get more accurate stresses in weldments by the finite element analysis, the converged finite element solutions could be considered with increasing the number of elements. However, since the models for this study have the same element aspect ratio and the stresses contributed by the mismatch are usually maximum at or very near the joint, the information obtained herein is believed to be all that is necessary for the parametric study purposes. Nevertheless, the

8

nonlinear analysis including both geometric and material nonlinearities might be necessary because the potentially critical locations with respect to the local stress raisers, for example, through sharp notches, weld metal porosity, slag or oxide inclusions, poor penetrations, shrinkage, weld surface roughness, etc., are expected to occur at the weld-parent metal interface. Also, if a change in curvature occurs at the mismatch, additional discontinuity stresses result. In this case, the mismatch stresses should be superimposed upon the geometrical discontinuity stresses from the curvature change and membrane stresses to obtain the total stress. In addition to these stresses from the geometry changes, since a weld inherently produces metallurgical notches, this metallurgical notch due mostly to the heat effect in the heat-affected zone also needs to be considered. Therefore, if the precise assessment for the specific design problems is needed in weld discrepancies, all of these factors might be necessary as a whole in the analysis. However, generally speaking, for the parametric study to see an effect of the influence of a specific parameter the present analysis models are considered to be fairly reasonable.

It should again be mentioned here that the present analysis results are applicable only to shells of constant thickness with a large ratio of radius-to-wall thickness, and stresses are found only at the junction. Finally, the information provided in this study should be of help in the selection of allowable amounts of mismatch for improving design and manufacture of the SSME HPFTP.
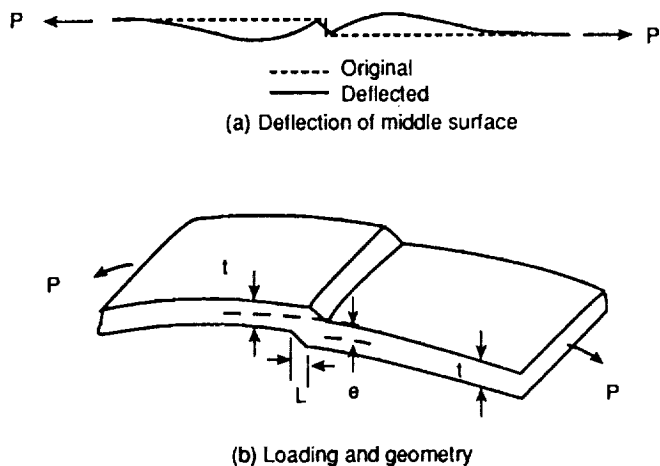

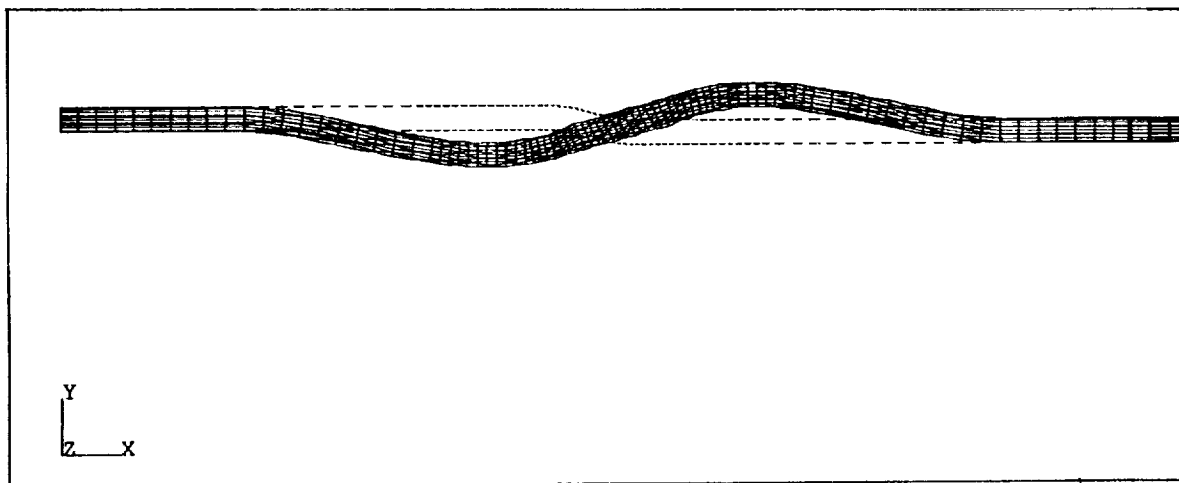Figure 1. Weld offset of longitudinally welded cylindrical structures [5].

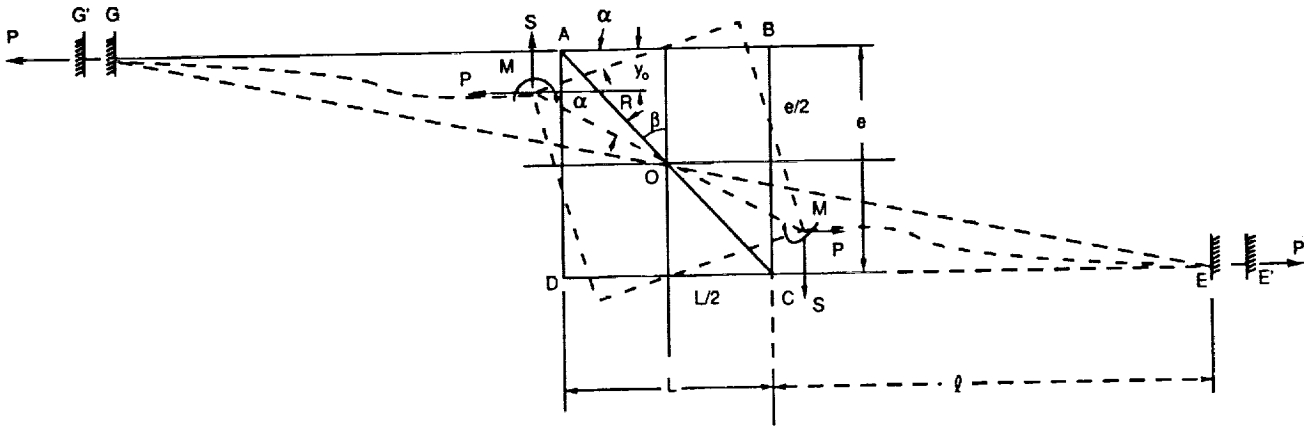Figure 2. Representative finite element model of weld offset.

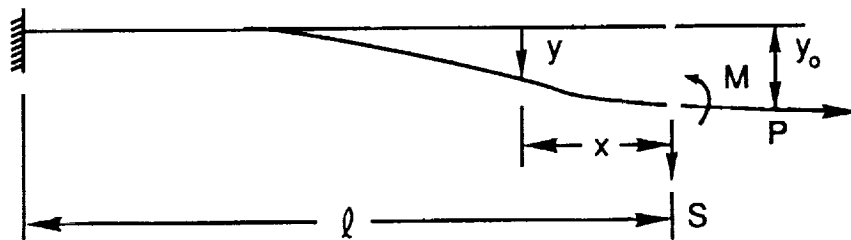Figure 3. Forces and moments on *ABCD* [3].

Figure 4. Assumed beam loadings [3].
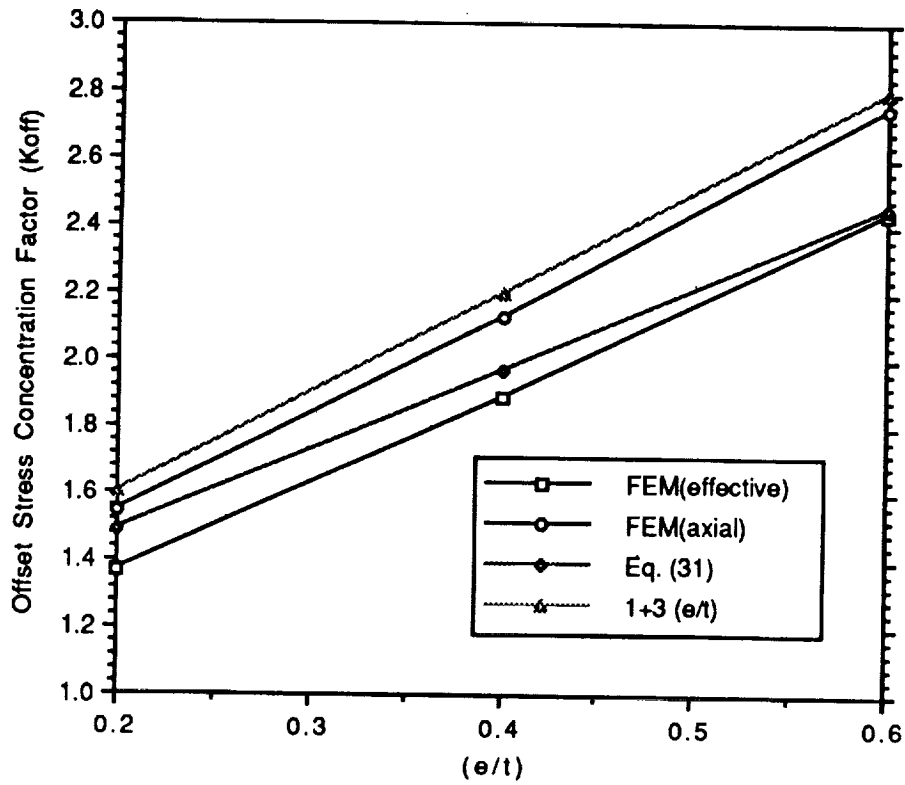
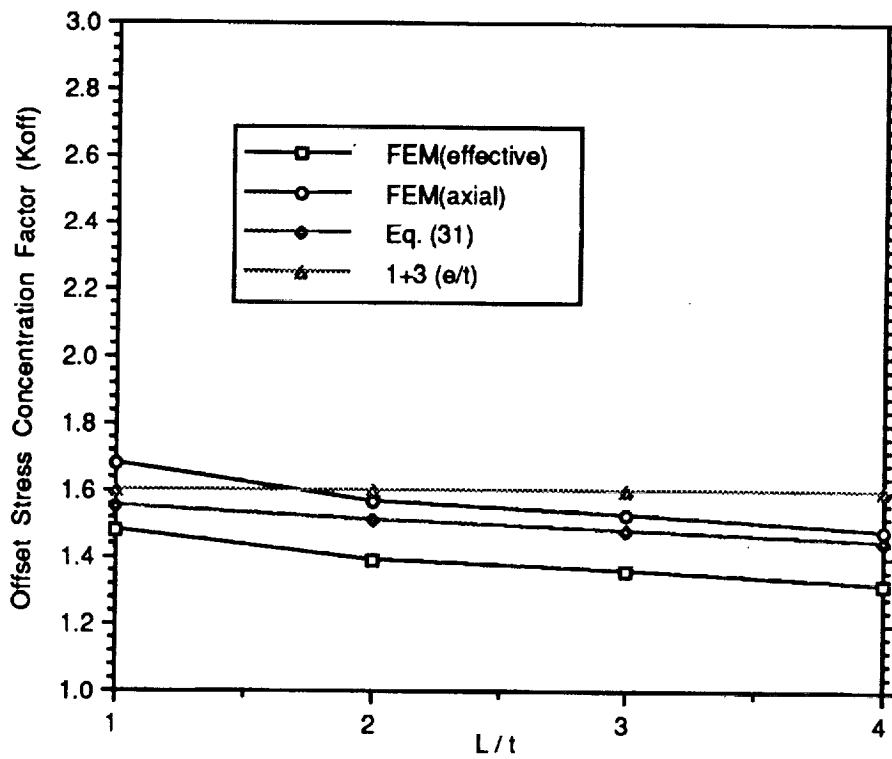10

Figure 5. $(e/t) = 0.2, 0.4, 0.6$ for $(L/t) = 2.86, \upsilon = 0.3$.

Figure 6. $(L/t) = 1, 2, 3, 4$ for $(e/t) = 0.2, \upsilon = 0.3$.

Figure 7. $(L/t) = 1, 2, 3, 4$ for $(e/t) = 0.4$, $\upsilon = 0.3$.

Figure 8. $(L/t) = 1, 2, 3, 4$ for $(e/t) = 0.6$, $\upsilon = 0.3$.

Figure 9. $(e/t) = 0.2, 0.4, 0.6$ for $(L/t) = 2.86$, $\upsilon = 0.0$.
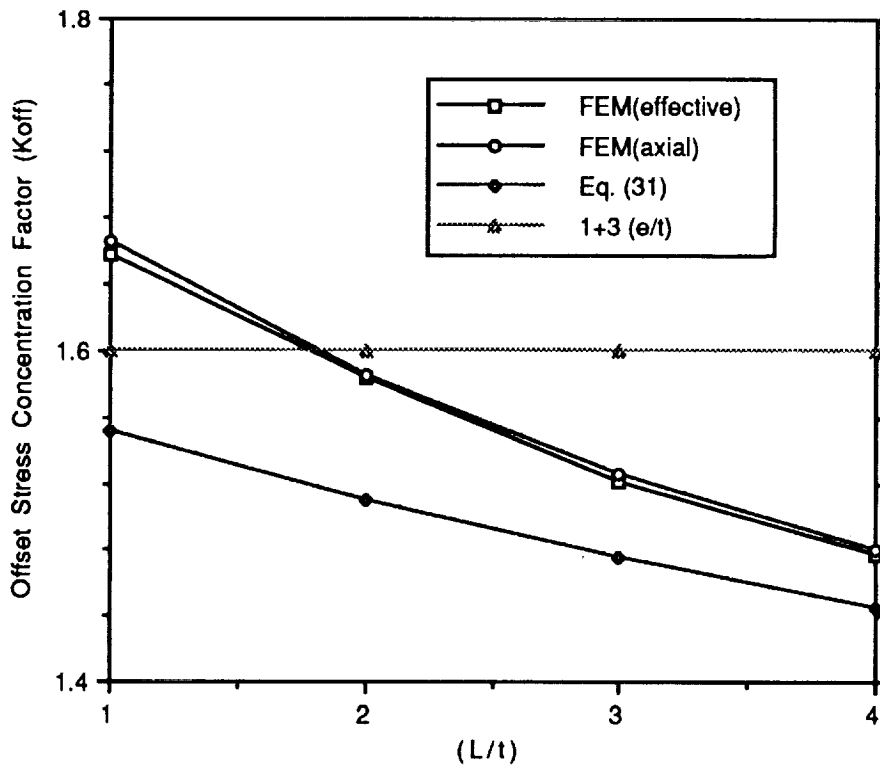
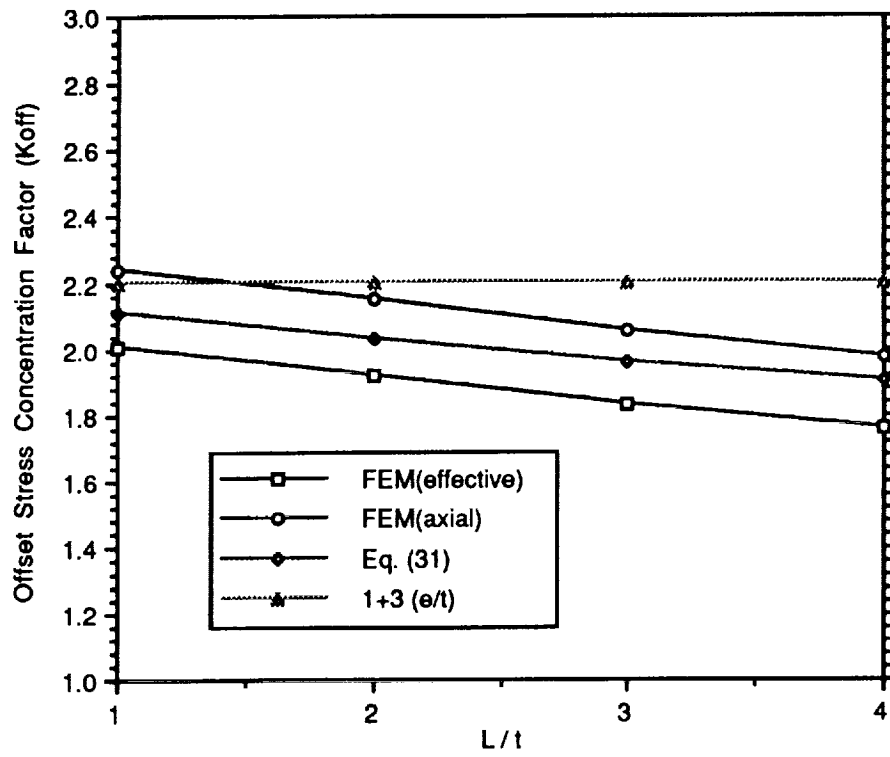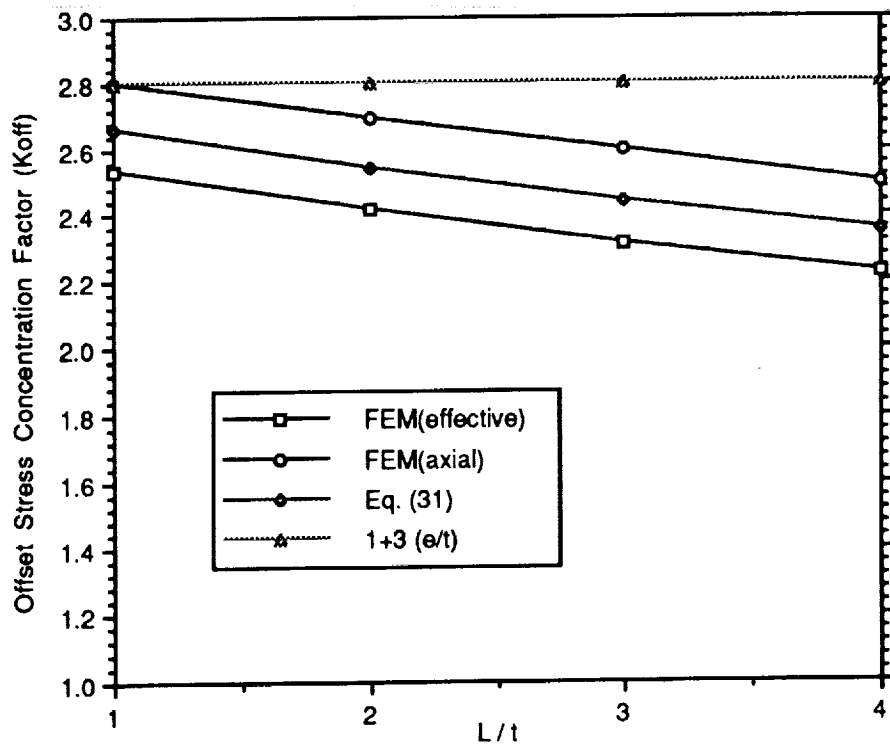Figure 10. $(L/t) = 1, 2, 3, 4$ for $(e/t) = 0.2$, $\upsilon = 0.0$.
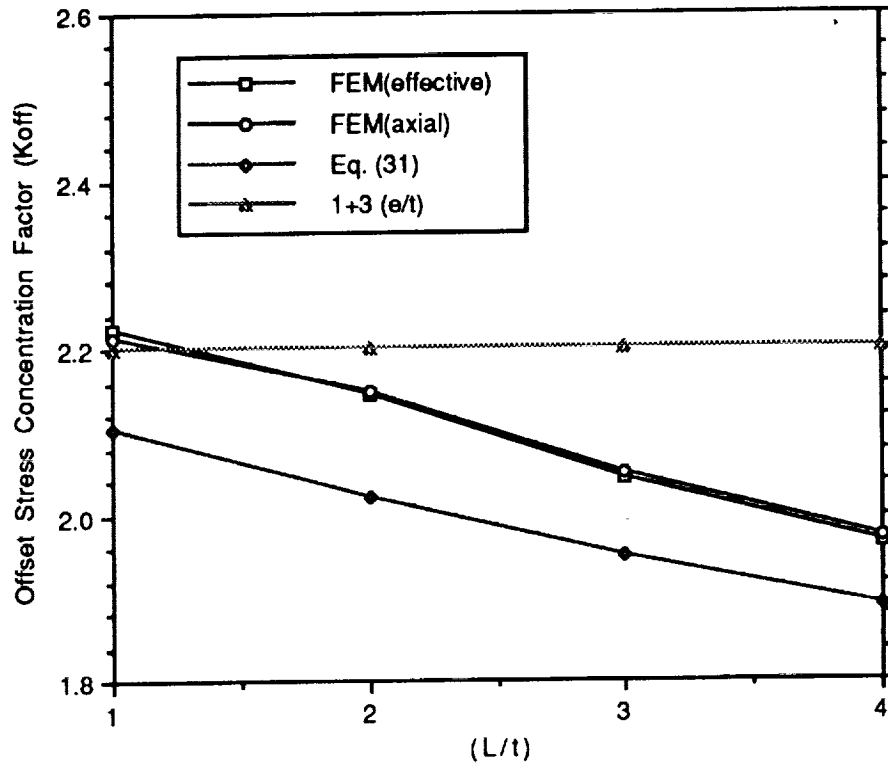
Figure 11. $(L/t) = 1, 2, 3, 4$ for $(e/t) = 0.4, \upsilon = 0.0$.

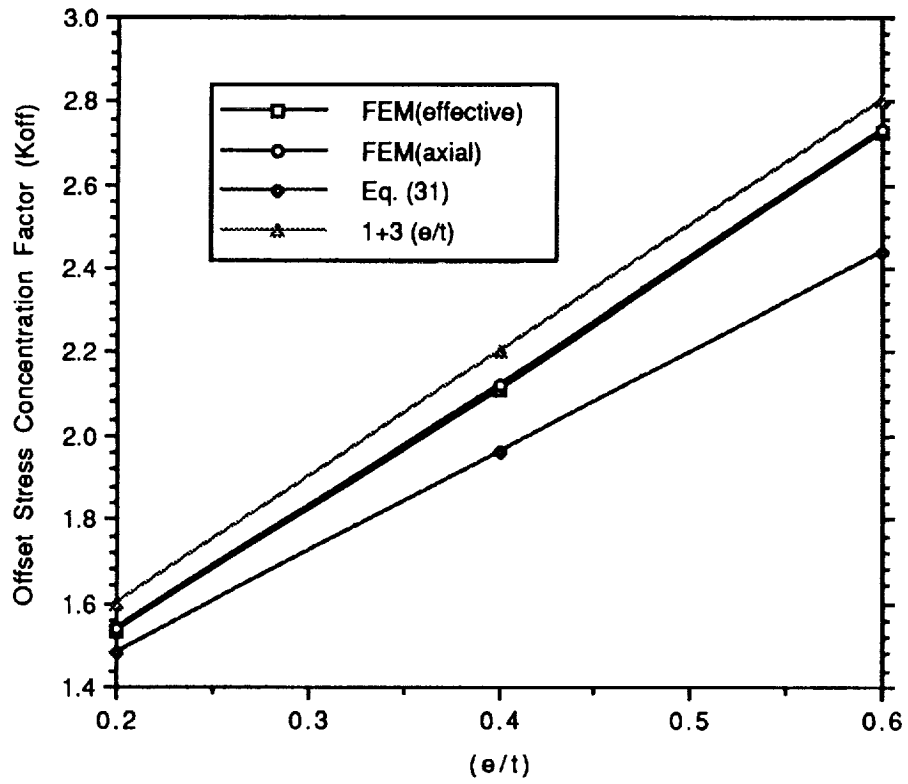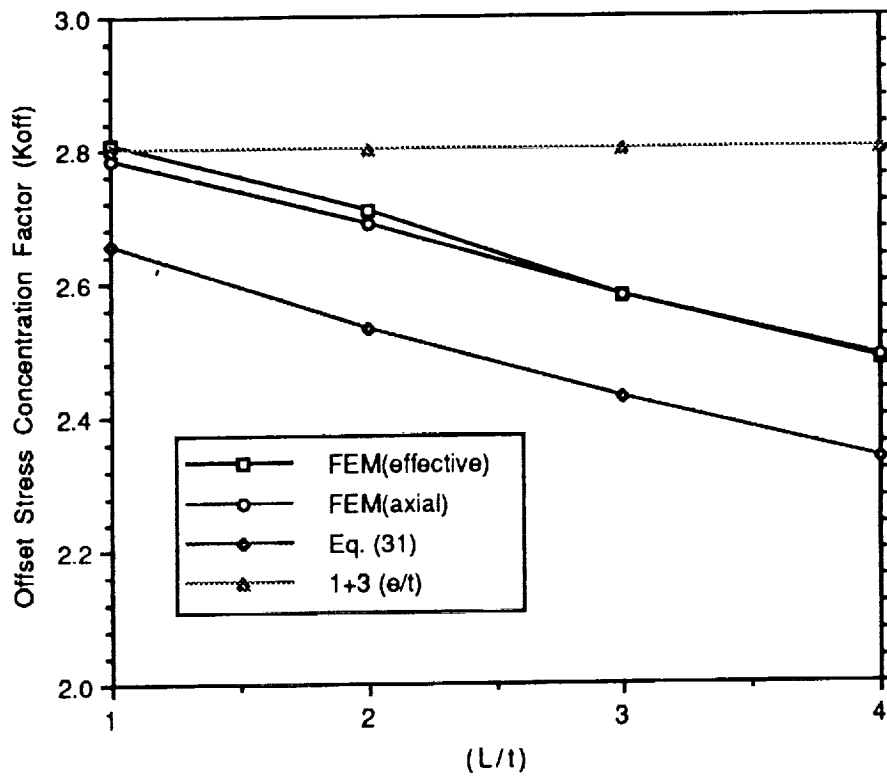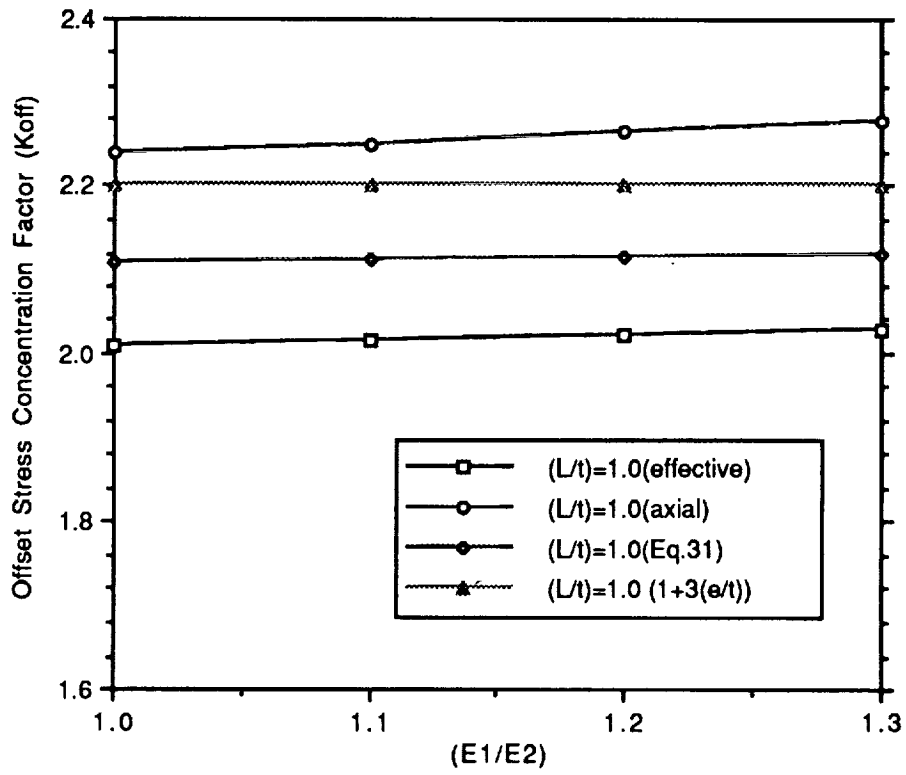Figure 12. $(L/t) = 1, 2, 3, 4$ for $(e/t) = 0.6, \upsilon = 0.0$.

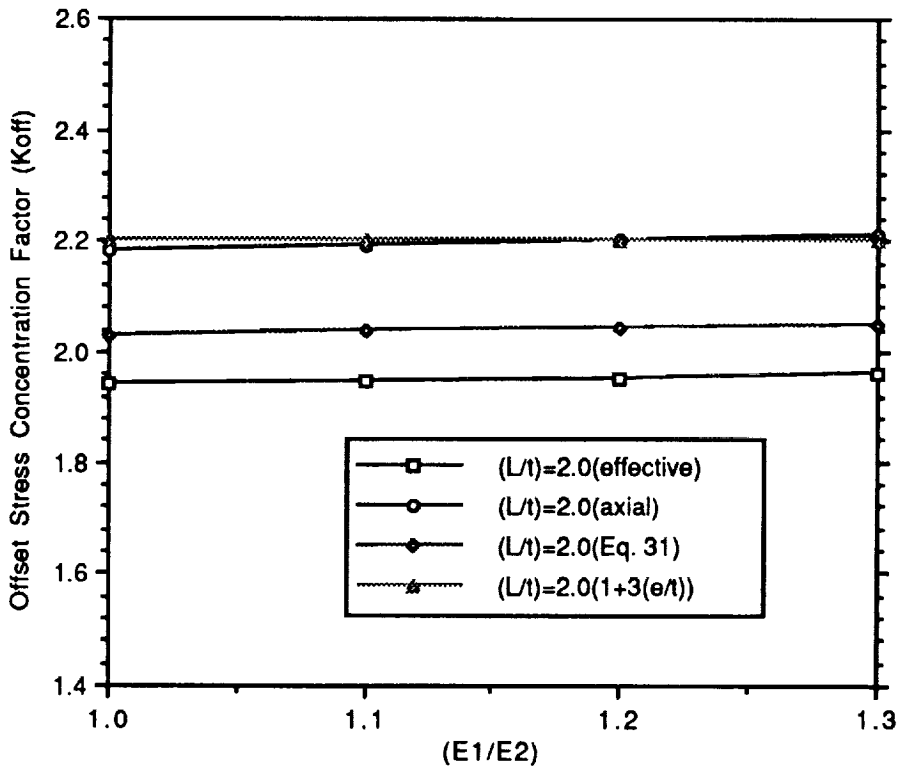Figure 13. (E_1/E_2) = 1.0, 1.1, 1.2, 1.3 for (L/t) = 1.0, υ = 0.3.

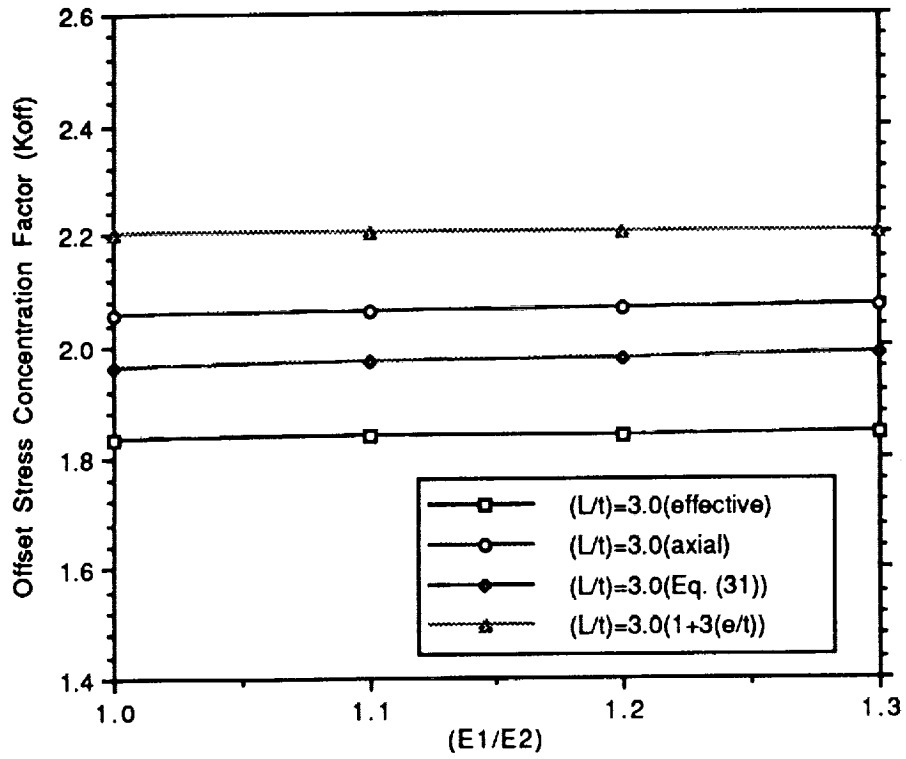Figure 14. (E_1/E_2) = 1.0, 1.1, 1.2, 1.3 for (L/t) = 2.0, υ = 0.3.

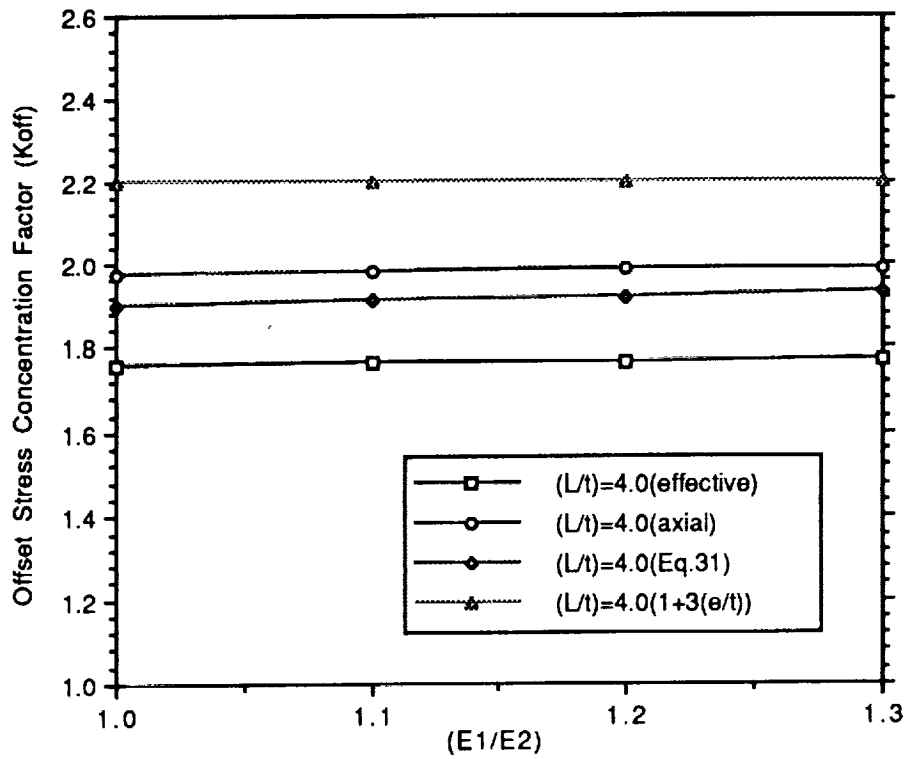Figure 15. (E_1/E_2) = 1.0, 1.1, 1.2, 1.3 for (L/t) = 3.0, υ = 0.3.

Figure 16. (E_1/E_2) = 1.0, 1.1, 1.2, 1.3 for (L/t) = 4.0, υ = 0.3.

16

Table 1. Data used in models.

Model #	L	e	t	L/t	e/t	υ	E1/E2
1	0.2	0.014	0.07	2.86	0.2	0.3	1.0
2	0.2	0.028	0.07	2.86	0.4	0.3	1.0
3	0.2	0.042	0.07	2.86	0.6	0.3	1.0
4	0.07	0.014	0.07	1.0	0.2	0.3	1.0
5	0.14	0.014	0.07	2.0	0.2	0.3	1.0
6	0.21	0.014	0.07	3.0	0.2	0.3	1.0
7	0.28	0.014	0.07	4.0	0.2	0.3	1.0
8	0.07	0.028	0.07	1.0	0.4	0.3	1.0
9	0.14	0.028	0.07	2.0	0.4	0.3	1.0
10	0.21	0.028	0.07	3.0	0.4	0.3	1.0
11	0.28	0.028	0.07	4.0	0.4	0.3	1.0
12	0.07	0.042	0.07	1.0	0.6	0.3	1.0
13	0.14	0.042	0.07	2.0	0.6	0.3	1.0
14	0.21	0.042	0.07	3.0	0.6	0.3	1.0
15	0.28	0.042	0.07	4.0	0.6	0.3	1.0
16	0.2	0.014	0.07	2.86	0.2	0.0	1.0
17	0.2	0.028	0.07	2.86	0.4	0.0	1.0
18	0.2	0.042	0.07	2.86	0.6	0.0	1.0
19	0.07	0.014	0.07	1.0	0.2	0.0	1.0
20	0.14	0.014	0.07	2.0	0.2	0.0	1.0
21	0.21	0.014	0.07	3.0	0.2	0.0	1.0
22	0.28	0.014	0.07	4.0	0.2	0.0	1.0
23	0.07	0.028	0.07	1.0	0.4	0.0	1.0
24	0.14	0.028	0.07	2.0	0.4	0.0	1.0
25	0.21	0.028	0.07	3.0	0.4	0.0	1.0
26	0.28	0.028	0.07	4.0	0.4	0.0	1.0
27	0.07	0.042	0.07	1.0	0.6	0.0	1.0
28	0.14	0.042	0.07	2.0	0.6	0.0	1.0
29	0.21	0.042	0.07	3.0	0.6	0.0	1.0
30	0.28	0.042	0.07	4.0	0.6	0.0	1.0
31	0.07	0.028	0.07	1.0	0.4	0.3	1.0
32	0.07	0.028	0.07	1.0	0.4	0.3	1.1
33	0.07	0.028	0.07	1.0	0.4	0.3	1.2
34	0.07	0.028	0.07	1.0	0.4	0.3	1.3
35	0.14	0.028	0.07	2.0	0.4	0.3	1.0
36	0.14	0.028	0.07	2.0	0.4	0.3	1.1
37	0.14	0.028	0.07	2.0	0.4	0.3	1.2
38	0.14	0.028	0.07	2.0	0.4	0.3	1.3
39	0.21	0.028	0.07	3.0	0.4	0.3	1.0
40	0.21	0.028	0.07	3.0	0.4	0.3	1.1
41	0.21	0.028	0.07	3.0	0.4	0.3	1.2
42	0.21	0.028	0.07	3.0	0.4	0.3	1.3
43	0.28	0.028	0.07	4.0	0.4	0.3	1.0
44	0.28	0.028	0.07	4.0	0.4	0.3	1.1
45	0.28	0.028	0.07	4.0	0.4	0.3	1.2
46	0.28	0.028	0.07	4.0	0.4	0.3	1.3

Table 2. Calculated weld offset stress concentration factors (K_{off}).

Model #	FEM(eff)	FEM(axial)	Eq. (31)	1+3 (e/t)
1	1.370	1.543	1.485	1.600
2	1.886	2.128	1.970	2.200
3	2.439	2.750	2.455	2.800
4	1.483	1.677	1.544	1.600
5	1.395	1.571	1.515	1.600
6	1.358	1.530	1.480	1.600
7	1.318	1.482	1.451	1.600
8	2.009	2.239	2.108	2.200
9	1.920	2.150	2.029	2.200
10	1.833	2.058	1.961	2.200
11	1.760	1.978	1.901	2.200
12	2.535	2.803	2.662	2.800
13	2.420	2.700	2.544	2.800
14	2.315	2.598	2.441	2.800
15	2.225	2.497	2.352	2.800
16	1.535	1.539	1.481	1.600
17	2.109	2.117	1.961	2.200
18	2.724	2.731	2.442	2.800
19	1.658	1.666	1.552	1.600
20	1.583	1.586	1.511	1.600
21	1.521	1.526	1.476	1.600
22	1.477	1.479	1.445	1.600
23	2.222	2.214	2.104	2.200
24	2.145	2.150	2.022	2.200
25	2.044	2.050	1.952	2.200
26	1.967	1.972	1.890	2.200
27	2.806	2.785	2.656	2.800
28	2.710	2.690	2.533	2.800
29	2.580	2.582	2.428	2.800
30	2.482	2.486	2.366	2.800
31	2.009	2.239	2.108	2.200
32	2.015	2.251	2.112	2.200
33	2.022	2.264	2.116	2.200
34	2.030	2.277	2.119	2.200
35	1.943	2.185	2.029	2.200
36	1.948	2.193	2.036	2.200
37	1.954	2.202	2.042	2.200
38	1.961	2.210	2.048	2.200
39	1.833	2.058	1.961	2.200
40	1.835	2.062	1.970	2.200
41	1.838	2.067	1.978	2.200
42	1.842	2.074	1.985	2.200
43	1.760	1.978	1.901	2.200
44	1.764	1.981	1.912	2.200
45	1.768	1.985	1.921	2.200
46	1.773	1.989	1.930	2.200

REFERENCES

1. Ugural, A.G.: "Stresses in Plates and Shells." McGraw-Hill Company, 1981.

2. ANSYS User's Manuals, Volumes I and II.

3. Sechler, E.E.: "Stress Rise Due to Offset Welds in Tension." Space Technology Laboratories, Inc., Report No. EM9-18, August 28, 1959.

4. Gunay, M.H.: Private Communications, Rocketdyne Division of Rockwell International Company.

5. Johns, R.H.: "Theoretical Elastic Mismatch Stresses." NASA Technical Note D-3254, January 1966.

APPROVAL

PARAMETRIC STUDY IN WELD MISMATCH OF LONGITUDINALLY WELDED SSME HPFTP INLET

By J.B. Min, K.L. Spanyer, and R.M. Brunair

The information in this report has been reviewed for technical content. Review of any information concerning Department of Defense or nuclear energy activities or programs has been made by the MSFC Security Classification Officer. This report, in its entirety, has been determined to be unclassified.

JAMES C. BLAIR
Director, Structures and Dynamics Laboratory